

# Strangeness production in fixed-target collisions at LHCb

Chiara Lucarelli<sup>1,\*</sup> on behalf of the LHCb collaboration

<sup>1</sup>INFN Firenze, Via Sansone, 1, 50019 Sesto Fiorentino (FI), Italy

**Abstract.** Studies of strangeness production in high-energy fixed-target collisions provide information on hadronization and serve as important inputs to models of particle production in cosmic rays. Thanks to its forward geometry and the possibility to inject gas into the beam pipe, the LHCb detector with the SMOG system is ideally suited to study strangeness production in fixed-target collisions at the LHC. We present recent LHCb results on strangeness production in fixed-target proton-nucleus collisions, including studies of hyperon production and polarization.

## 1 Introduction

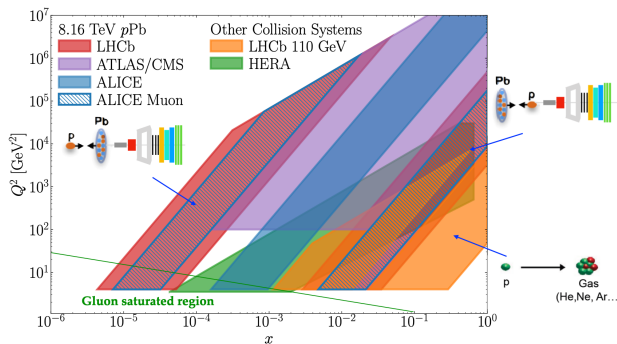


**Figure 1.** The LHCb acceptance in the  $Q^2$ /Bjorken- $x$  plane compared to other experiments.

The LHCb experiment is a single-arm forward spectrometer covering the pseudorapidity range between  $2 < \eta < 5$  [1]. Originally designed to study heavy hadrons produced in  $pp$  collisions at the LHC, it has proven during the 2011-2018 data-taking years to be a general purpose experiment in the forward direction. Among the experiments operating at the LHC, LHCb has the unique ability to inject gases in the accelerator beam-pipe, a feature originally conceived to exploit the proton-gas collisions in order to reconstruct the LHC beam transverse profiles and measure the luminosity. Since 2015, leveraging on the forward geometry of the detector and its excellent particle reconstruction and identification performance, the gas injection system SMOG has also been used as a gaseous target, turning LHCb into the highest-energy fixed-target experiment ever. During Run 2, samples with both proton and lead ion beams were collected injecting noble gases (He, Ne, Ar),

\*e-mail: chiara.lucarelli@cern.ch

covering a rapidity region in the centre of mass system ( $-3 < y^* < 0$ ) complementary to the ones covered by the collider mode samples. This configuration provides unique physics opportunities at the LHC. The high Bjorken- $x$  and moderate  $Q^2$  region, mostly unexplored by previous experiments, can be accessed with SMOG and collision systems with atomic numbers between the proton and lead can be studied, providing inputs to many research fields such as heavy flavour production, nuclear structure and cosmic rays astrophysics (Fig. 1) [2].

## 2 $\bar{p}$ production from antihyperon decays in $p$ He collisions at $\sqrt{s_{NN}} = 110$ GeV

The antimatter abundance in cosmic rays is a sensitive probe for indirect dark matter searches. Space-based experiments, such as AMS-02, have been measuring the antimatter flux and have highlighted possible discrepancies with the spectra expected from the production in cosmic rays spallation with the interstellar medium, mainly composed of hydrogen and helium. However, the interpretation of these results is still limited by our knowledge of the antimatter production in known processes [3]. Exploiting the injection of helium through SMOG, LHCb performed the first-ever measurements of prompt antiproton ( $\bar{p}$ ) production in  $p$ He collisions at  $\sqrt{s_{NN}} = 110$  GeV, contributing to improvements of the modelling of secondary  $\bar{p}$  production in space [4]. The non-prompt  $\bar{p}$  contribution originating from anti-hyperon decays, called "detached", has been addressed in a separate measurement [5]. The detached-to-prompt  $\bar{p}$  production ratio has been measured using two complementary approaches, exploiting the prompt result in the ratio. In the exclusive approach, the dominant contribution coming from the  $\bar{\Lambda} \rightarrow \bar{p}\pi^+$  is reconstructed by exploiting the secondary vertex topology without the use of any particle identification information. A second inclusive approach considers the detached  $\bar{p}$  from all anti-hyperon species. The  $\bar{p}$  candidates are identified using the Ring Imaging Cherenkov detectors, and the prompt and detached contributions are determined based on each candidates consistency with originating from the  $p$ He collision point. The dominant uncertainty due to the luminosity cancels out in the ratio in both cases. Both approaches highlight a larger contribution in the ratio with respect to the predictions of the most commonly used theoretical models. The results will contribute to reducing the uncertainty on the secondary  $\bar{p}$  production cross-section in the collisions between the cosmic rays and the interstellar medium (Fig. 2).

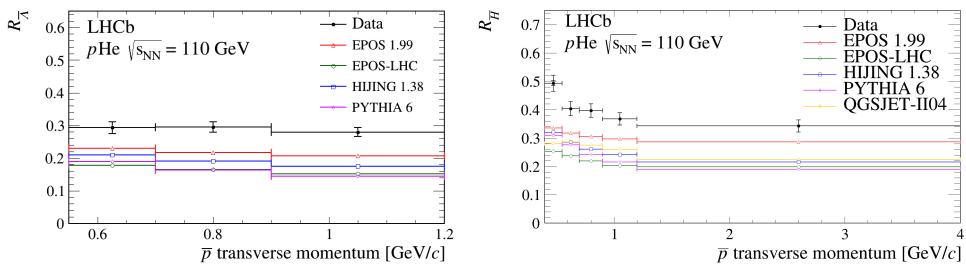


**Figure 2.** Results for the detached-to-prompt antiproton ratio measurement as a function of the transverse momentum. Both the exclusive (left) and inclusive (right) approaches show an excess with respect to the predictions.

### 3 $\Lambda$ transverse polarization in $p$ Ne collisions at $\sqrt{s_{NN}} = 68.4$ GeV

The spontaneous transverse polarization of  $\Lambda$  hyperons was first observed in 1976 in inclusive production by an unpolarized 300 GeV proton beam on a beryllium target [6]. While several mechanisms are under study to explain the polarized production of the *Lambda* in collisions involving nuclei, as of today, the polarization in light systems has been generally explained through the introduction of transverse-momentum-dependent (TMD) fragmentation functions. In particular, the polarizing fragmentation function  $D_{1T}^\perp$  describes the fragmentation of an unpolarized quark into a transversely polarized hadron accounting for spin and momentum correlations [7]. Given that the determination of TMD fragmentations is based on experimental data, several experiments have been performed to try to describe the  $\Lambda$  polarization. LHCb performed the  $\Lambda$  transverse polarization measurement considering the  $p$ Ne sample at  $\sqrt{s_{NN}} = 68.4$  GeV [8]. The decays of the  $\Lambda \rightarrow p\pi^-$  and  $\bar{\Lambda} \rightarrow \bar{p}\pi^+$  are exploited to measure the polarization. Given the strong parity violation of these decays, the angular distribution of the products show a large asymmetry. Considering the  $\Lambda$  rest frame, the proton is preferentially emitted along the direction of the  $\Lambda$  spin and the magnitude of the polarization is obtained from the linear fit to the angular distribution of the proton. The final polarization obtained are  $P_\Lambda = 0.029 \pm 0.019$  (stat)  $\pm 0.012$  (syst) and  $P_{\bar{\Lambda}} = 0.003 \pm 0.023$  (stat)  $\pm 0.014$  (syst) for the  $\Lambda$  and  $\bar{\Lambda}$ , respectively. The results as a function of the x-Feynman variable  $x_F$  have also been compared with previous experiments (Fig. 3). Even though the results cover a wide range in the kinematics and collisions systems, the polarization obtained is in agreement with previous measurements, in particular with the HERA-B results, which cover a similar  $x_F$  region.

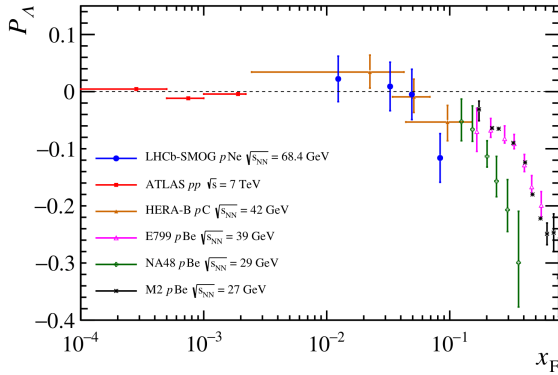


**Figure 3.** Comparison of the magnitude of the  $\Lambda$  hyperon polarization as a function of  $x_F$  obtained in the experiments performed up to the time of writing.

### 4 LHCb fixed-target Run3 upgrade

In preparation for the LHC Run 3, which began in 2022, the LHCb detector went through an upgrade, and a new gas injection system, SMOG2, was installed [9]. It consists of a 20 cm-long storage cell installed 44 cm upstream of the nominal LHCb interaction point and a new gas feed system that allows a fine and automatic control of the gas flow, pressure, and injected species. The confined interaction region allows for a two-orders-of-magnitude increases in instantaneous luminosity, and new non-noble gases, such as hydrogen ( $H_2$ ), deuterium ( $D_2$ ) and oxygen ( $O_2$ ), can be injected. Moreover, the separation of the beam-beam and beam-gas interaction regions makes it possible to acquire data from both types of collisions simultaneously, making LHCb the first experiment running at the same time with two different interaction systems and collision energies. The first physics data have been collected during may 2024 with all available gases, recorded simultaneously with  $pp$  collisions [10]. Figure 4

shows the recorded integrated luminosity during May 2024, as well as an example of the invariant mass distribution of reconstructed  $\Lambda \rightarrow p\pi^-$  candidates in the data-taking periods with simultaneous  $pp + p\text{Ne}$  collisions. While the data acquisition lasted 2 hours, more than twenty millions  $\Lambda$  candidates were reconstructed. A very large sample of charm hadrons can therefore be expected from the SMOG2 system. The upgraded fixed-target system will therefore contribute to a “significant extension of the LHC complex physics reach at a limited cost”, as highlighted in the 2020 European Strategy for Particle Physics Update [11].

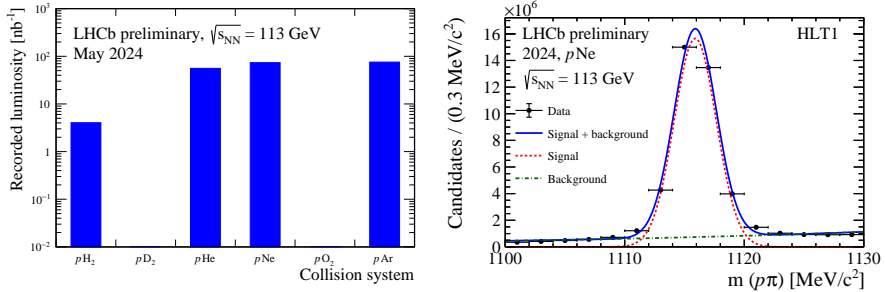


**Figure 4.** The left plot shows the integrated luminosity recorded during May 2024, corresponding to around two hours of injections per gas. The right plot shows the invariant mass distribution for  $\Lambda \rightarrow p\pi^-$  decay candidates.

## References

- [1] Aaij, R. et al., The LHCb Detector at the LHC. *Journal of Instrumentation* **3**, 08 S08005 (2008). [10.1088/1748-0221/3/08/S08005](https://doi.org/10.1088/1748-0221/3/08/S08005)
- [2] Bursche, A. et al., Physics opportunities with the fixed-target program of the LHCb experiment using an unpolarized gas target. [CERN-LHCb-PUB-2018-015](https://arxiv.org/abs/1808.01515) (2018).
- [3] Giesen, G. et al., AMS-02 antiprotons, at last! Secondary astrophysical component and immediate implications for Dark Matter. *JCAP* **09**, 023 (2015). [10.1088/1475-7516/2015/09/023](https://doi.org/10.1088/1475-7516/2015/09/023)
- [4] Aaij, R. et al., Measurement of Antiproton Production in  $p\text{He}$  Collisions at  $\sqrt{s_{\text{NN}}} = 110$  GeV. *Phys. Rev. Lett.* **121**, 22 222001 (2018). [10.1103/PhysRevLett.121.222001](https://doi.org/10.1103/PhysRevLett.121.222001)
- [5] Aaij, R. et al., Measurement of antiproton production from antihyperon decays in  $p\text{He}$  collisions at  $\sqrt{s_{\text{NN}}} = 110$  GeV. *Eur. Phys. J. C* **83**, 6 543 (2023). [10.1140/epjc/s10052-023-11673-x](https://doi.org/10.1140/epjc/s10052-023-11673-x)
- [6] Bunce, G. et al.,  $\Lambda^0$  Hyperon Polarization in Inclusive Production by 300-GeV Protons on Beryllium. *Phys. Rev. Lett.* **36**, 19 1113–1116 (1976). [10.1103/PhysRevLett.36.1113](https://doi.org/10.1103/PhysRevLett.36.1113)
- [7] Boer, D. et al., Spin asymmetries in jet-hyperon production at LHC. *Physics Letters B* **659**, 1 127-136 (2008). [10.1016/j.physletb.2007.10.059](https://doi.org/10.1016/j.physletb.2007.10.059)
- [8] Aaij, R. et al., Transverse polarization measurement of  $\Lambda$  hyperons in  $p\text{Ne}$  collisions at  $\sqrt{s_{\text{NN}}} = 68.4$  GeV with the LHCb detector. Submitted to *JHEP* (2024). [arXiv:2405.11324](https://arxiv.org/abs/2405.11324)
- [9] Boente Garcia, O., A high-density gas target at the LHCb experiment. Submitted to *Physical Review Accelerators and Beams* (2024). [arXiv:2407.14200](https://arxiv.org/abs/2407.14200)
- [10] Aaij, R. et al., First results from SMOG2 2024. [LHCb-FIGURE-2024-005](https://arxiv.org/abs/2407.14200) (2024).
- [11] Ellis, R. K. et al., Physics Briefing Book: Input for the European Strategy for Particle Physics Update 2020. [CERN-ESU-004](https://arxiv.org/abs/1907.02637) (2019).